The Holocene 16,8 (2006) pp. 1043–1057

East-Asian monsoon variability between 15 000 and 2000 cal. yr BP recorded in varved sediments of Lake Sihailongwan (northeastern China, Long Gang volcanic field)

Georg Schettler,[1*] Qiang Liu,[2] Jens Mingram,[1] Martina Stebich[3] and Peter Dulski[1]

([1]GeoForschungsZentrum Potsdam, Telegrafenberg, D-14473 Potsdam, Germany; [2]Institute of Geology and Geophysics, Chinese Academy of Sciences, 100029 Beijing, China; [3]Senckenberg Forschungsstation für Quartärpaläontologie, Am Jakobskirchhof 4, D-99423 Weimar, Germany)

Received 28 November 2005; revised manuscript accepted 22 May 2006

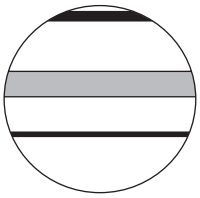

Abstract: A palaeohydrological reconstruction on decadal scale for the period 15 000–2000 cal. yr BP based on calculated net accumulation rates for biogenic silica (F-bSiO_2) and additional proxies (sedimentological data, geochemical sediment characteristics and pollen) is derived from varved sediments of Lake Sihailongwan (SHL). In Lake SHL, F-bSiO_2 is positively correlated with the inflow of nutrient-rich groundwater. Since groundwater inflow is mainly fed by seepage of summer monsoon rainfall, F-bSiO_2 documents changes in summer monsoon strength. Summer monsoon rainfall was enhanced in the early Holocene around 9800 and 7800 cal. yr BP. Groundwater inflow during these periods did not reach the high level of the Lateglacial warm period (*c.* 14 300–12 500 cal. yr BP) when the vicinity of the lake was less densely covered with woody vegetation than in the Holocene. Aeolian influx of silt-sized debris was relatively higher during an overall drier period between 9500 and 8000 cal. yr BP. A mid-Holocene sedimentation interval with distinct century-scale variability in summer monsoon rainfall documents a positive correlation between rainfall and siliciclastic influx that reflects a more efficient removal of mineral aerosols for increased rainfall at an overall high dust concentration over the Asian continent. Summer monsoon rainfall reached minima around 6400, 4900, 3700 and 2200 cal. yr BP. Remarkably, aeolian siliciclastic influx peaked at the beginning and at the end of a dry interval between 4100 and 3600 cal. yr BP. Around 3600 cal. yr BP Lake SHL received substantial aeolian influx of different geochemical provenance.

Key words: Palaeoclimate, East-Asian monsoon, lacustrine sediments, sediment geochemistry.

Introduction

Atmospheric circulation in East Asia is characterized by large-scale seasonal changes of the wind regime. Zonal westerlies of the mid latitudes, Walker and tropical Hadley circulation superimpose wind shifts at the surface, which are forced by the temperature contrast between the Asian land mass and the subtropical western Pacific Ocean. In winter, near surface, northwesterlies prevail, upper westerlies (jet stream) split into two currents to the north and south of the Tibetan Plateau (Barry and Chorley, 1998). Dust transport from arid areas in Inner Asia is conventionally associated with the strength of the winter monsoon (intensity of northwesterlies). Mineral aerosols can rise in higher troposheric levels and can be transported far into the Pacific Ocean. Between spring and summer, the southern branch of the jet stream gradually shifts northwards, which results in strengthening of the upper westerlies north of the Tibetan Plateau. During the summer monsoon East China receives inflow of moist Pacific air masses from the subtropical

*Author for correspondence (e-mail: schet@gfz-potsdam.de)

10.1177/0959683606069388

and tropical Pacific. Rainfall in north-central and northeastern China is mainly associated with the summer monsoon and shows high interannual variability. It occurs by the interaction of northwest-moving moist Pacific air (summer monsoon front) with northern cooler air masses (subpolar front). The rainfall belt migrates discontinuously northward and commonly reaches northeast China in July. The discontinuous progression of the summer monsoon front is strongly influenced by the dislocation of subtropical anticyclones over the western Pacific (Domrös and Peng, 1988). The moisture load of the inflowing Pacific air masses is positively correlated with the surface sea water temperature (SST) and should principally increase by a northern shift of the Intertropical Convergence Zone (ITCZ). The temperature contrast between the Asian continent and the subtropical western Pacific is a major forcing factor for the inflow intensity of moist Pacific air during the summer monsoon. The encroachment of the summer monsoon front, however, is among others influenced by the tropical Hadley circulation, and the seasonal retreat of the subpolar front. The strength of the tropical Hadley circulation in summer, which determines the subtropical High in southeast China, depends on the SST of the tropical western Pacific and is influenced by the Walker circulation (ENSO connection, eg, Hu, 1997; Kumar *et al*., 1999). Variations in the East-Asian monsoon regime are still not satisfactorily understood because of the complex interactions between the above-mentioned factors.

Present knowledge about palaeovariations of the East-Asian monsoon is based on various kinds of geological data, including marine (eg, Kudrass *et al*., 1991) and terrestrial records (lacustrine and peat records, tree ring data, speleothem data and loess/palaeosol profiles). These data, as partially referred by An *et al*. (2000), Morrill *et al*. (2003) and Wang *et al*. (2005), document a general humidity increase for northeast Asia during the Lateglacial period by the spread of deciduous broadleaf forest. Lake level reconstructions from northeast China (a1–a4, Figure 1; An *et al*., 2000), document that lake level stands were highest between *c*. 14 000 and 12 000 cal. yr. BP, reflecting a generally higher precipitation/evaporation ratio than for the following period. A Younger Dryas-like climatic deterioration is among others documented in speleothem records (Hulu cave: Wang *et al*., 2001; Dongge cave: Dykoski *et al*., 2005), and in a lacustrine record from southern China (Lake Huguang: Mingram *et al*., 2004a) and Japan (Nakagawa *et al*., 2002, 2003) (see Figure 1 for locations). Around 9000 cal. yr BP, the obliquity, periohelion and eccentricity constellation was associated with a 7.2% higher solar radiation for July at mid-northern latitudes compared with modern values (Kutzbach, 1981 and references therein). This potentially strengthens summer monsoon circulation by increased heating of the Asian land mass (see also Bush, 2005, for orbitally driven monsoon variability). Climate models (eg, Bush, 2001), however, demonstrate that SST development in the tropical and subtropical western Pacific cannot be disregarded as an equally important forcing factor. Knowledge of the East-Asian monsoon variability during the Holocene is still incomplete. Recent reviews of palaeoclimatic records from various parts of China stress the asynchrony of Holocene climate development in China (eg, He *et al*., 2004) and point to implications for abrupt changes of the East-Asian summer monsoon circulation during the Holocene. Huang *et al*. (2004), for instance, argue that the decline of rain-fed cereal agriculture on the Loess Plateau after *c*. 4000 cal. yr BP was caused by distinctly decreased summer monsoon rainfall.

Annual laminated sediments of maar and crater lakes from the Quaternary Long Gang volcanic field represent highly resolved terrestrial archives for palaeovariations of the East-Asian monsoon regime (Mingram *et al*., 2004b). They trap atmospheric deposition of mineral aerosols and document changes in regional hydrological conditions that are closely associated with interannual variations of rainfall during the summer monsoon. In a preliminary study, we investigated sedimentation in Lake Sihailongwan over the last 200 years (Schettler *et al*., 2006a,b). Lake Sihailongwan does not receive inflow from tributaries and has no outlet. It is fed mainly by rainfall during the summer monsoon (see Table 1 for morphometric and hydrological characteristics, and Schettler *et al*., 2006a, for hydrochemical data). Local rainfall between May and October accounts for *c*. 85% of annual precipitation. The interior of the SHL crater is covered with coarse easily weatherable pumic tuff of alkalibasaltic composition that became mixed with siliciclastic particles of remote provenance by continued aeolian deposition. The coarse pyroclastics favour seepage of rain, furthermore, dense mixed conifer-deciduous forest in the lake catchment is associated with high evapotranspiration, which together minimizes soil erosion by surface runoff. Reconstructed flux rates of atmospheric ^{210}Pb, biogenic silica and Al_2O_3 document a positive correlation between summer monsoon rainfall, groundwater inflow and wet deposition of dust over the last *c*. 200 years. Low inwash of local debris and focusing of the particle flux make the annual laminated sedimentation record from the centre of the U-shaped SHL lake basin a sensitive monitor for aeolian influx and for changes in autochthonous biogenic deposition. Though water residence time in the lake is rather high (*c*. 30 years), the SHL sediments sensitively document the external forcing on autochthonous biogenic production, since nutrient-rich groundwater, fed by summer monsoon rainfall, discharges into the nutrient-depleted phototrophic zone of the lake during summer stratification. Sediment trap data (Chu *et al*., 2005) document peaks in the depositional flux of diatomaceous matter during spring and autumn overturn, and increasing diatom production from July to the end of September associated with groundwater inflow during the rainy season. Investigation of SHL sediments offered the possibility to quantify and to characterize aeolian influx from remote sources in Inner Asia in the context of the derived summer monsoon variability for northeast China.

Sampling and methods

Sediment cores were recovered by Usinger piston core technique from the centre of the lake during a field campaign in summer 2001. Overlapping 2-m drives from a total of three adjacent coring sites at the centre of the lake basin enabled us to establish continuous composite profiles. Permanent cooling of the sediments was ensured from the field to the laboratory. In the GFZ laboratories, sediments were extruded, cut in half along their length axis, and photographed for documentation.

Petrographic thin sections have been prepared for the entire sediment profile of lake SHL, using the freeze-drying method described by Merkt (1971). Analysis of seasonal sedimentation and varve counting is based on thin-section observations using predominantly polarized light (to enhance the minerogenic components) and dark field illumination (to enhance diatom enrichments).

We subsampled continuously 1-cm sediment slices (1cm × 4cm × 3cm) from the centre of the half cores for chemical and sedimentological analyses. Sediment samples were freeze-dried and then dry sieved (200 μm) for homogenization. The remaining coarse fractions accounted for insignificant portions

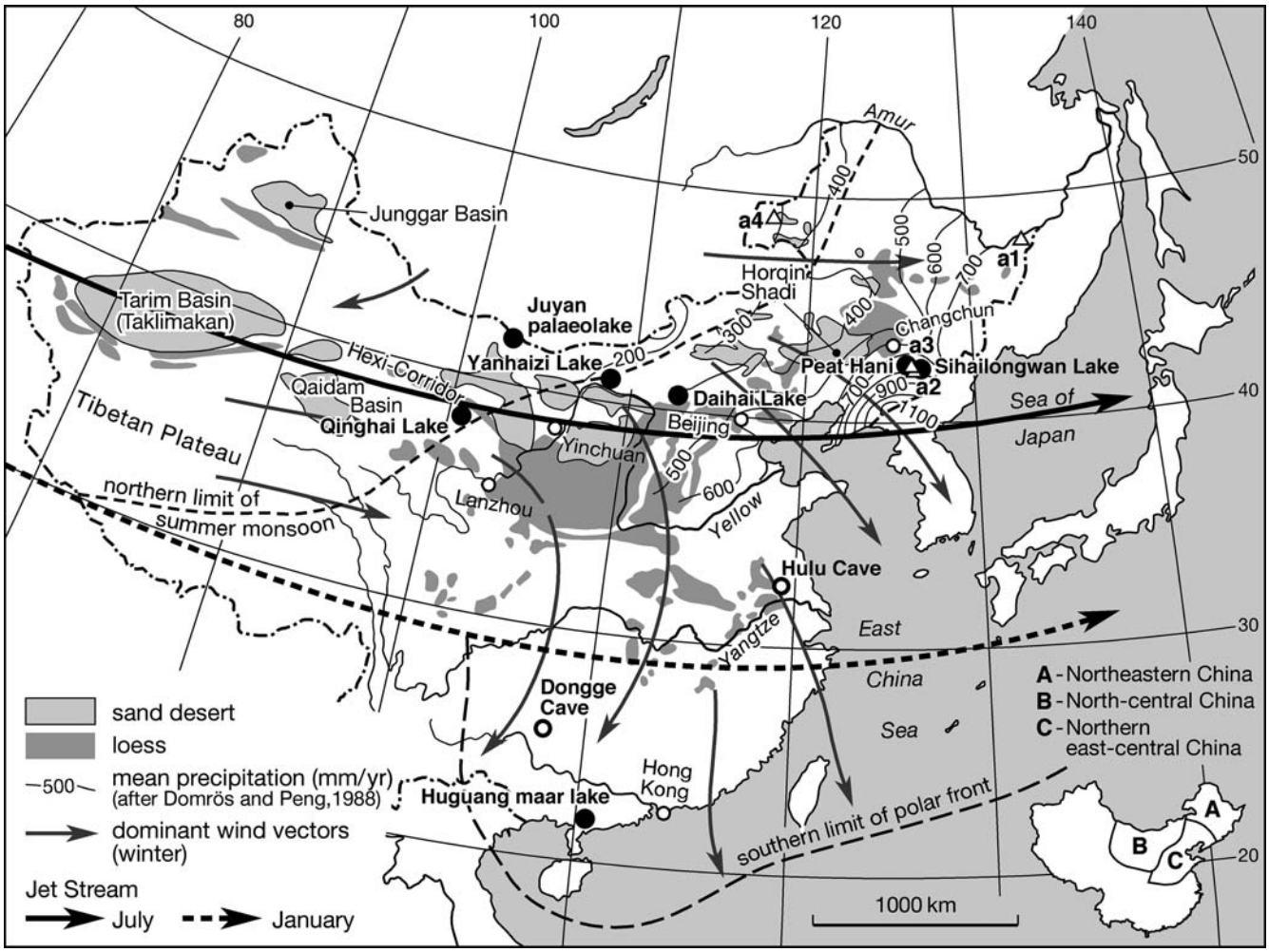

Figure 1 Overview map, showing selected elements of atmospheric circulation over East Asia and possible source regions of aeolian influx into Lake SHL. The Long Gang volcanic field and palaeoclimatic records referred to in the paper are marked on the map. a1, Qingdeli, 48°00′N 133°15′E, 52 m a.s.l.; a2, Jingchuan, 42°20′N 126°22′E, 600 m a.s.l.; a3, Gushantun, 42°30′N 126°10′E, 600 m a.s.l.; a4, Hulun Lake 49°00′N 117°20′E, 540 m a.s.l. (source: An *et al.*, 2000: table 1). Subdivision into East-Asian monsoon regions after An *et al.* (2000), modern summer monsoon limit redrawn after Gao *et al.* (1962)

of the total sample dry weights. Water contents were determined by the weight difference before and after freeze-drying. The density of the solid sediment (ρ_s) was measured by means of a He-pycnometer (Micromeritics, Accu Pyc 1330). The standard deviation of repeated measurements typically varied between 0.0002 and 0.002 g/cm^3. Sediment porosity was determined based on measured water contents and density values of the solid sediment. Major and trace element analysis, determination of inorganic carbon (IC), total organic carbon (TOC), total nitrogen (N) and biogenic silica (soda-leachable Si fraction) was carried out as described in Schettler *et al.* (2006a,b). The remaining siliciclastic residue after leaching with soda was carefully washed with diluted HCl and deionized water, and separated from clay-sized particles by repeated centrifugation (1000 r.p.m., 1 min). Complete separation from clay-sized particles was checked by laser-particle analysis for selected samples. The siliciclastic sediment fraction, thus derived, consisted of nearly 100% silt (< 63 μm) and allows us to estimate the silt fraction of the bulk detrital input. Soda-leachable silica contents of 16 soil and loess samples were determined by the same procedure to estimate possible contributions by leaching of siliciclastic sediment constituents. The leachable SiO_2 content of these samples typically varied between 1 and 2 wt% (Schettler *et al.*, 2006a). Calculation of mean mass accumulation rates (SR_m) is based on the counted varve number per 1-cm sample, measured ρ_s values and derived porosity values. SR_m and elemental flux rates are distinctly enhanced for sediment sections with several millimetre-thick macroscopically visible graded layers originating from aeolian input during dust storm events, inwash by surface runoff, or

Table 1 Morphological and hydrological data

Modern Lake Sihailongwan	
Location	42°17′N, 126°36′E
Elevation	797 m (a.s.l.)
Maximum depth	50 m
Diameter	720 m
Lake surface area	$4.07 \cdot 10^5$ m^2
Lake volume	$9.5 \cdot 10^6$ m^3
Water residence time	*c.* 36 yr
Catchment area	*c.* $7.0 \cdot 10^5$ m^2
Max. elev. crater-rim	918 m (a.s.l.)
Precipitation:	
Mean (NDJFMA)	114 mm
Mean (MJJASO)	661 mm
Air temperatures:	
Mean (Jan)	−18.1°C
Mean (July)	20.7°C

Data on precipitation and mean temperature given for the period between 1955 and 1997. Source: Meteorological Station of Jingyu.

re-suspension of surface sediments, respectively. The 1-cm samples of such sections inadequately describe the geochemical composition of the graded layers and the flux rates of 'normal' sedimentation in the related intervals. The total siliciclastic sediment constituent All^{total} is estimated for assumed constant Al_2O_3 concentration of the detritus influx. The silt/Al_2O_3 ratio is calculated to estimate possible variations in the grain size composition of the siliciclastic sediment constituent. Since the Al_2O_3 concentration of clay-sized debris exceeds the Al_2O_3 content of silt in SHL sediments (Schettler *et al.*, 2006a), this proxy sensitively records variations in the silt/clay ratio of the detrital influx.

Lithology and chronology

Sediments of Lake SHL are almost continuously seasonally laminated. Annual laminae are varves of mixed organogenic/minerogenic composition (Mingram *et al.*, 2004b). According to varve composition diatom frustules represent the dominant contributor to the biogenic silica content of Lake SHL sediments throughout the last 14 500 years. Minor contributions by stomatocysts of Chrysophyte algae are present (less than 5% of the total count of microfossils back to 12 800 cal. yr BP: Patrick Rioual, personal communication, 2006). Stomatocyst types 202, 266 and 351 could be detected in sediment trap materials of the modern lake (Chu *et al.*, 2005). Particularly during the Lateglacial, annual laminations are interrupted by the occurrence of graded event layers. Holocene sediments document two major local volcanic eruptions at 2019 (T1) and 10 461 (T2) varve yr BP; T1 (9 cm) represents a vitric tuff of alkalibasaltic composition, T2 (14 cm) originates from a phreatomagmatic eruption with an alkalibasaltic vitric tuff (major constituent) and lithoclasts from the granite basement. Sediments have been varve-counted for the entire Lateglacial and Holocene. Additionally, 36 AMS ^{14}C datings, almost entirely based on terrestrial plant macrofossils, have been performed (Table 2). Calibration of AMS ^{14}C ages has been done with CALIB Radiocarbon Calibration program, version 5.0.2 (Reimer *et al.*, 2004). Calibrated radiometric AMS ^{14}C ages and derived varve ages show a continuously increasing difference with depth (Table 2). The deficit in varve counts reflects randomly distributed uncertainties in the identification of varves along the sediment profile. There are no specific sediment horizons with generally poor varve preservation. We therefore applied a constant factor for the correction of varve ages. The considered correction factor of 1.0622 represents the slope of the regression line in the plot of corresponding varve ages and calibrated AMS ^{14}C ages. All ages given in the text and figures for SHL sediments represent varve ages derived from original thin-section varve counting corrected by multiplication with 1.0622.

Results and discussion

Major geochemical sediment signatures *(Figure 2)*

The biogenic sediment fraction of the nearly non-calcareous SHL sediments (AU^{total}), which mainly originates from autochthonous production, is roughly estimated by $AU^{total} = bSiO_2 \cdot 2.2$ (see Figure 2a for contributions by $bSiO_2$, TOC, N) and is characterized by a distinct lower solid density (ρ_s) than the allochthonous sediment constituent (All^{total}). All^{total} estimates that consider an Al_2O_3 concentration of 16 wt% for the siliciclastic sediment constituent closely correspond with All^{total} estimates by: $100 - bSiO_2 \cdot 2.2$ (Figure 2b). Discrepancies between the estimates for some Lateglacial and early Holocene sedimentation intervals are associated with a high abundance of *Pediastrum* and/or relatively lowered contributions by terrestrial organic matter (Figure 2b,c,h). Below 570 cm (> 14 300 varve yr BP) All^{total} accounts for *c.* 90% of the bulk sediment (Figure 2b). Sediments between 570 and 523 cm (14 300–14 000 varve yr BP) show rapidly increasing contributions by AU^{total} (Figure 2a). The proportion of AU^{total} gradually decreases afterwards and remains at a low level until 423 cm (11 700 varve yr), when it increases again. The density of the solid sediment and the profile of $Al_2O_3/bSiO_2$ document changes in the ratio between autochthonous biogenic production and siliciclastic influx (Figure 2d,e); $Al_2O_3/bSiO_2$ was distinctly enhanced at: 12 500–11 500, 11 000–10 600 and 9500–8500 varve yr BP. The nearly non-calcareous SHL sediments show slightly enhanced carbonate contents before 13 800 and between 12 500 and 11 500 varve yr BP (Figure 2f). In the SHL sediments, TOC and $bSiO_2$ as major components of AU^{total} typically show a mass ratio close to 1 (Figure 2g). Lateglacial and early Holocene sediments with enhanced $bSiO_2$ concentrations are characterized by TOC/$bSiO_2$ ratios of $\sim$0.5. The overall high TOC/N documents substantial contributions from terrestrial plant remnants for most of the sedimentation record (Figure 2h). Particularly, in early Holocene sediments with enhanced $bSiO_2$, TOC/N declines close to 10. This reflects higher contributions from planktonic organic matter.

Lateglacial sedimentation

The pollen spectra of Lake SHL reveal the widespread occurrence of open birch woodland-grassland vegetation at the study site between 15 000 and 13 600 varve yr BP (Stebich *et al.*, 2007). A strong rise in the total pollen concentration at *c.* 14 300 varve yr BP reflects climatic development towards warmer and moister summer conditions. At the same time, the thermophile broadleaf taxa *Ulmus* and *Fraxinus* began to gradually occupy the study area. At 13 600 varve yr BP, a rapid spread of broadleaved forests mainly composed of *Ulmus* and *Fraxinus* occurred (Figure 3c,d). Final transformation of Lateglacial woodland types into dense deciduous forests similar to the recent situation (arboreal pollen > 80%), however, was first established after *c.* 11 100 varve yr BP.

The derived very high accumulation rates of biogenic silica (F-$bSiO_2$) for Lateglacial sedimentation between *c.* 14 300 and 12 500 varve yr BP (Figure 3b) reflect (i) substantial amounts of rainfall, (ii) high groundwater inflow because of lower evapotranspiration (EVPT) in the lake catchment, (iii) high $bSiO_2$ burial at up to ten times higher annual mass accumulation (SR_m), in combination with a higher focusing factor of the settling particle flux at an overall higher lake level. Furthermore, young glacial soils may have sustained a high release rate of nutrients into percolating precipitation. Distinct flux peaks frequently occurring in Lateglacial and early Holocene sediments (Figure 3a,b) are associated with graded layers.

Re-appearance of *Picea* and *Larix* between *c.* 12 500 and 11 500 varve yr BP, coupled with a marked decrease of *Ulmus* and *Fraxinus*, implies climatic deterioration during a Younger Dryas-like period. F-$bSiO_2$ values of this sedimentation interval decline on the level of sediments deposited before 14 300 varve yr BP and siliciclastic influx is distinctly enhanced (Figure 3a–c). Sediments of the section are characterized by generally higher $Al_2O_3/bSiO_2$ ratios, a higher density of the solid sediment, slightly enhanced carbonate contents, and short-term fluctuations of TOC/N (Figure 2d–f,h). Occurrence of graded layers in this sedimentation interval may reflect siliciclastic input by surface runoff, which may have been favoured by freezing of the ground. Surface sediments may

Table 2 SHL chronology data composite profile 1

Lab. code[a]	Material	Depth (cm)	Radiometric data				Varve ages	
			AMS ^{14}C yr BP	Uncertainty ±yr	cal. yr BP 2σ-range	cal. yr BP median	Varve counts before 1950	Corrected varve yr BP[b]
KIA 8097	leaf	45.0	525	25	511–624	568	633	672
KIA 8098	leaf	47.0	335	32	309–478	394	669	711
V18452	wood	77.5	1313	40	1173–1302	1238	1289	1369
V18453A	leaf	97.0	1784	41	1573–1821	1697	1741	1849
Poz-5432	leaf	98.0	1725	35	1548–1711	1630	1761	1871
V18454	leaf	118.8	2128	42	1992–2304	2148	2063	2191
Poz-10349	leaf	128.0	2450	30	2359–2702	2530	2345	2491
V18455	leaf	147.0	2917	43	2929–3214	3072	2889	3069
V18456	leaf	163.0	3362	51	3464–3719	3592	3372	3582
Poz-5429	leaf	165.3	3460	50	3587–3852	3719	3456	3671
Poz-10377	leaf	172.2	3655	33	3891–4085	3988	3658	3886
V18457	leaf	178.5	3910	46	4160–4511	4336	3848	4087
Poz-10378	seed	186.5	4080	35	4440–4809	4624	4071	4324
Poz-5430	seed	194.5	4170	40	4577–4835	4706	4330	4599
Poz-5431	leaf	194.5	(3350)[c]	(120)	–	–	–	–
V18458	leaf	198.5	4375	55	4840–5272	5056	4457	4734
Poz-10350	leaf	214.1	4745	35	5328–5586	5457	4999	5310
Poz-10351	leaf	225.4	5060	40	5669–5911	5790	5370	5704
V18459	leaf	237.8	5604	50	6299–6480	6390	5774	6133
Poz-5428	leaf	251.5	6030	50	6742–7002	6872	6294	6686
V18466A	leaf	262.5	6279	55	7013–7319	7166	6701	7118
V18467	leaf	290.0	7407	76	8045–8374	8210	7625	8099
Poz-10352	leaf	306.9	7990	50	8649–9007	8828	8243	8756
V18460	leaf	318.5	8520	110	9153–9886	9520	8585	9119
Poz-10368	seed	357.0	9180	60	10 234–10 500	10 367	9662	10 263
V18461A	leaf	362.8	9059	67	9931–10 412	10 172	9832	10 440
Poz-10344	moss	385.75	9650	70	10 767–11 202	10 984	9994	10 616
Poz-10353	leaf	386.0	9590	50	10 741–11 144	10 942	9997	10 619
V18465A	seed	408.9	9927	63	11 216–11 618	11 417	10 604	11 264
V18462	wood	424.3	10 243	72	11 650–12 362	12 006	11 033	11 719
Poz-5434	moss	451.75	10 240	80	11 623–12 376	11 999	11 573	12 293
Poz-10354	leaf	465.6	10 930	70	12 815–13 000	12 908	11 979	12 724
V18463	leaf	466.7	10 980	150	12 747–13 208	12 998	12 012	12 759
V18464	leaf	481.0	10 818	97	12 657–12 956	12 806	12 336	13 103
Poz-10355	moss	565.0	12 330	80	14 003–14 759	14 381	13 430	14 265
Poz-10346	wood	615.2	13 290	70	15 384–16 170	15 777	14 392	15 287

[a]KIA, Leibniz-Labor for Radiometric Dating and Isotope Research, Kiel, Germany; V18, Arizona University, USA; Poz, Poznán Radiocarbon Laboratory, Poland.
[b]Age values used in text.
[c]Sample too small, age value not considered.

have become exposed to erosion by lake level lowering as a result of climate variation. The flux of $bSiO_2$ shows substantial re-increase as a result of climate amelioration at around 11 500 varve yr BP and century-scale variability during the following 1500 years. The F-$bSiO_2$ record is affected by fall-out of a 14-cm thick tephra layer (T2) at 10 461 varve yr BP (Figure 3b). We therefore refrain from a detailed discussion of this sedimentation interval.

Further geochemical implications for groundwater inflow variations

Trace elements with low concentrations in the major mineral constituents of the siliciclastic input and high mobility can be used to infer variations in the groundwater inflow. Uranium and molybdenum, which form oxy-anions, in principle, fulfil the above conditions. Co-precipitation and scavenging of U and Mo in the lake and within the aquifer depends among others on redox conditions. We use the conservative major element Al for normalization to estimate variations in the dissolved influx of Mo and U (Mo^{exc}, U^{exc}); considered $Mo(U)/Al_2O_3$ ratios for the detrital input are 0.03 and 0.17, respectively (ratios given in ppm/wt%). These values represent the lowest $Mo(U)/Al_2O_3$ ratios obtained in siliciclastic SHL sediments deposited before 14 300 varve yr BP. Considered Mo and U concentration values for the detrital input are 0.5 and 2.7 ppm, respectively. These values are typical for the silt fraction of loess-like sediments and sand dunes NW of the Long Gang volcanic field (G. Schettler, unpublished data). Easily weatherable alkalibasaltic pumic tuff may be the main contributor to the dissolved influx of Mo and U. The concentration range of 12 alkalibasaltic tephra samples from the interior of the SHL crater is 0.9–1.7 ppm for U and 0.8–3.3 ppm for Mo. The atomic concentration of Mo in local alkalibasaltic tephra exceeds that of U about 4.4 times. Furthermore, U is substantially associated with stable heavy minerals, whereas Mo is largely hosted in the glass of the tuff particles, which is less resistant to chemical alteration. It can therefore be expected that groundwater inflow variability is more sensitively recorded by the Mo^{exc} influx. The derived Mo^{exc} flux (F-Mo^{exc}) accounts for *c.* 90% of the total Mo input. It reaches maximum values of 1 mg/m^2 per yr during the Lateglacial and around 10 600 varve yr BP and gradually

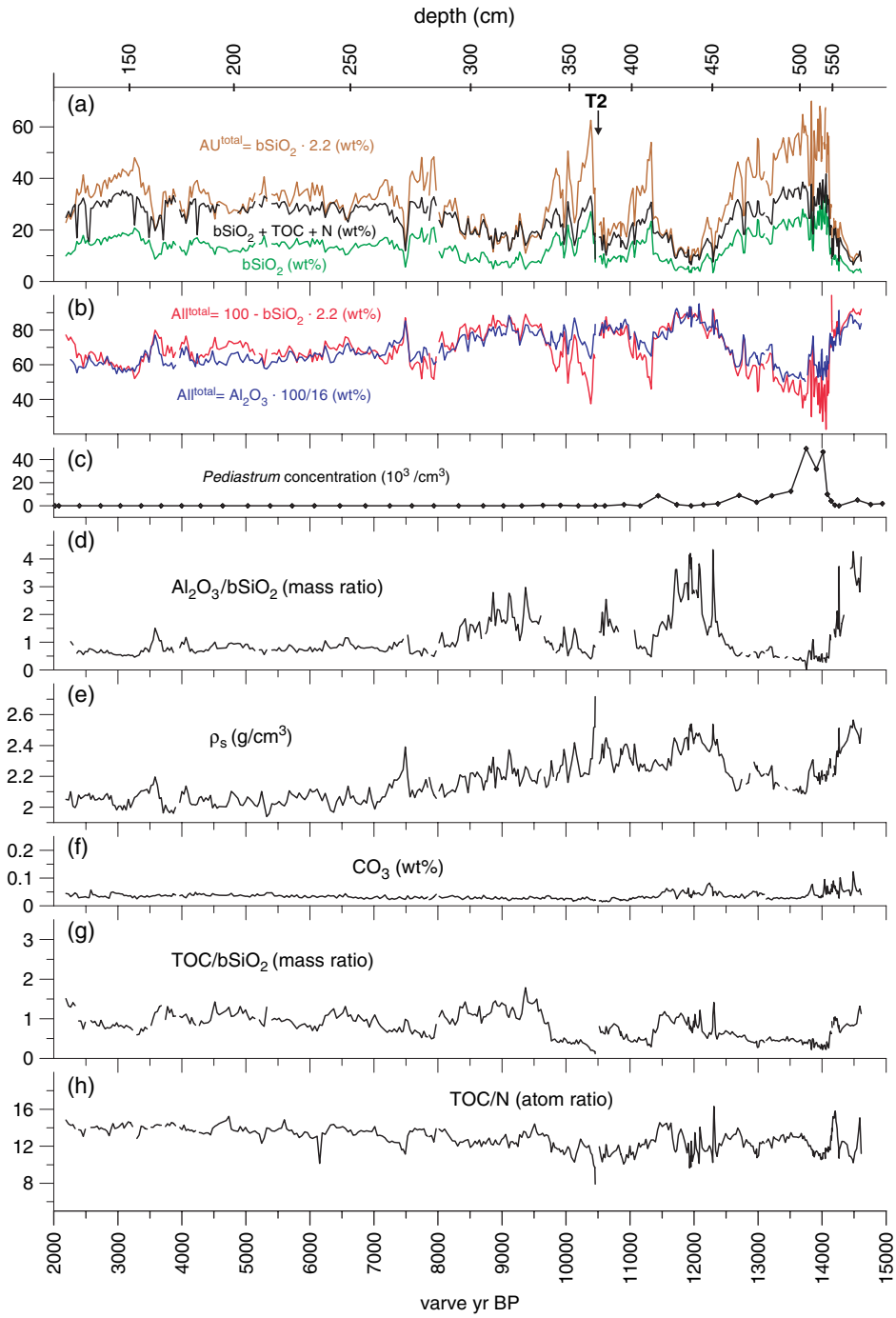

Figure 2 Major geochemical characteristics of Lateglacial and Holocene SHL sediments

declines to 0.3 mg/m^2 per yr for sedimentation after 6900 varve yr BP (Figure 4a). Reduced groundwater inflow during climatic deterioration between 12 500 and 11 500 varve yr BP is clearly documented in the F-Mo^{exc} profile.

Molybdate is less particle-reactive than U(VI). Deposition of dissolved MoO_4^{2-} is significantly enhanced under anoxic conditions by reaction with H_2S (Vorlicek *et al.*, 2004; Tribovillard *et al.*, 2004 and numerous references therein). The latter explains the coincidence of narrow F-Mo^{exc} and F-S^{total} peaks (Figure 4a,b). In general, significant H_2S production is not sustained by the low SO_4 concentration of Lake SHL (Schettler *et al.*, 2006a). Enhanced lake productivity during the Lateglacial warming and during some sedimentation intervals in the early Holocene, as documented by the flux profiles of S^{total} (Figure 4b) and $bSiO_2$ (Figure 3b), is associated with increased oxygen consumption in the deep water. The TOC/S^{total} profile (Figure 4c) implies that the net flux of sulphur decreased gradually until *c.* 6500 varve yr BP, since oxic conditions in the deep water were sustained increasingly longer during the stratification periods. In combination with reduced biogenic uptake of Mo, this should have resulted in an overall decreasing transfer efficiency for dissolved Mo into the sediment and a longer residence time of Mo in the lake water.

Dissolved transport of U released by chemical weathering is not favoured by the formation of carbonate complexes in percolating rainfall because of the non-calcareous character of the catchment; U(VI) can be scavenged by Fe-oxidhydroxids (eg, Bruno *et al.*, 1995; Davis *et al.*, 2004) or is immobilized as U(IV) in the organic-rich top soils. Uranium is not irreversibly scavenged. Climatic amelioration during the Lateglacial around 14 300 varve yrs BP and the re-increase of the summer monsoon strength after 11 500 varve

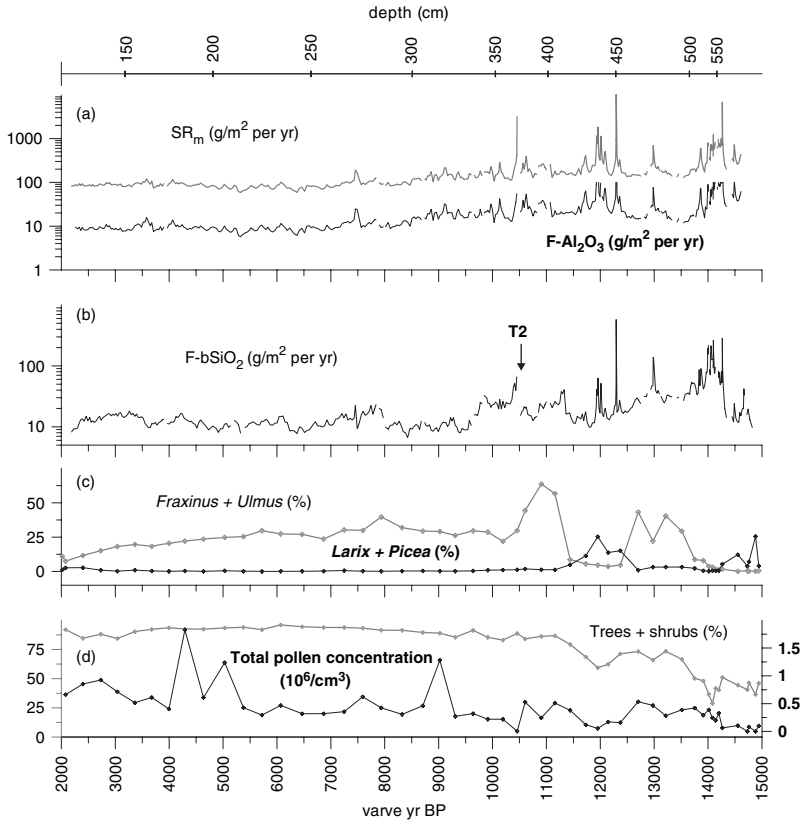

Figure 3 (a), (b) Mean annual mass accumulation (SR_m) and flux rates of Al_2O_3 and $bSiO_2$. (c), (d) Selected pollen data, redrawn after Stebich *et al.*, 2007

yr BP are geochemically marked by U/Al_2O_3 peaks (Figure 4d). The U/Al_2O_3-peaks probably document leaching of U that was scavenged in the dry periods previously. The pool of leachable U should be positively correlated with the duration of dry climatic conditions that explains the less pronounced U/Al_2O_3 peak at around 11 400 varve yr BP. Dissolved U influx ($F\text{-}U^{exc}$) immediately increased with Lateglacial climatic amelioration around 14 300 varve yr BP and reached its maximum between 14 200 and 13 900 varve yr BP when it accounted for up to 90% of the total U input (Figure 4e,f). $F\text{-}U^{exc}$ decreased by 10% of $F\text{-}U^{total}$ after 12 500 varve yr BP and only temporarily increased by a higher proportion in response to climatic amelioration after 11 500 varve yr BP.

Holocene sedimentation

11 500–8000 varve yr BP

The $F\text{-}Mo^{exc}$ profile (Figure 4a) implies that, in the course of the climatic amelioration, groundwater inflow reached a

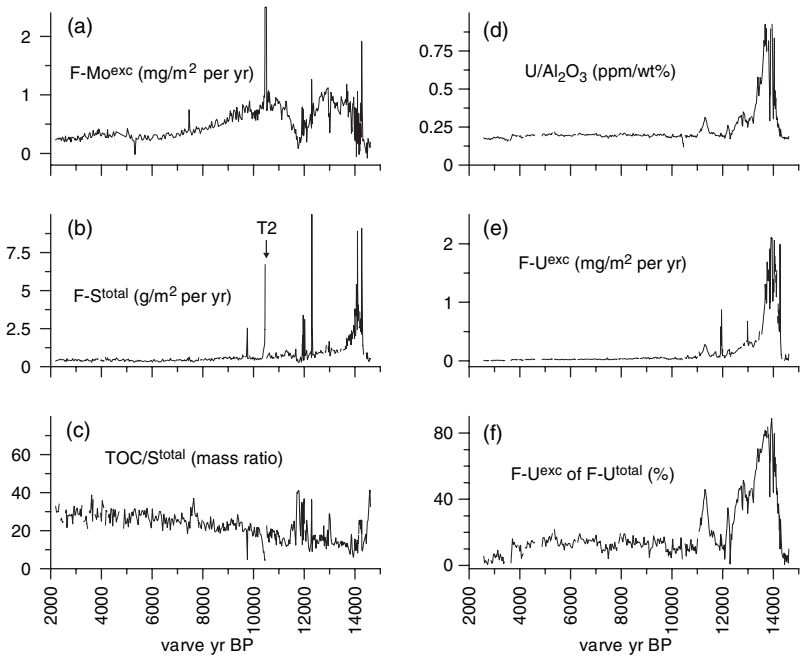

Figure 4 Selected elemental flux rates and geochemical signatures of SHL sediments

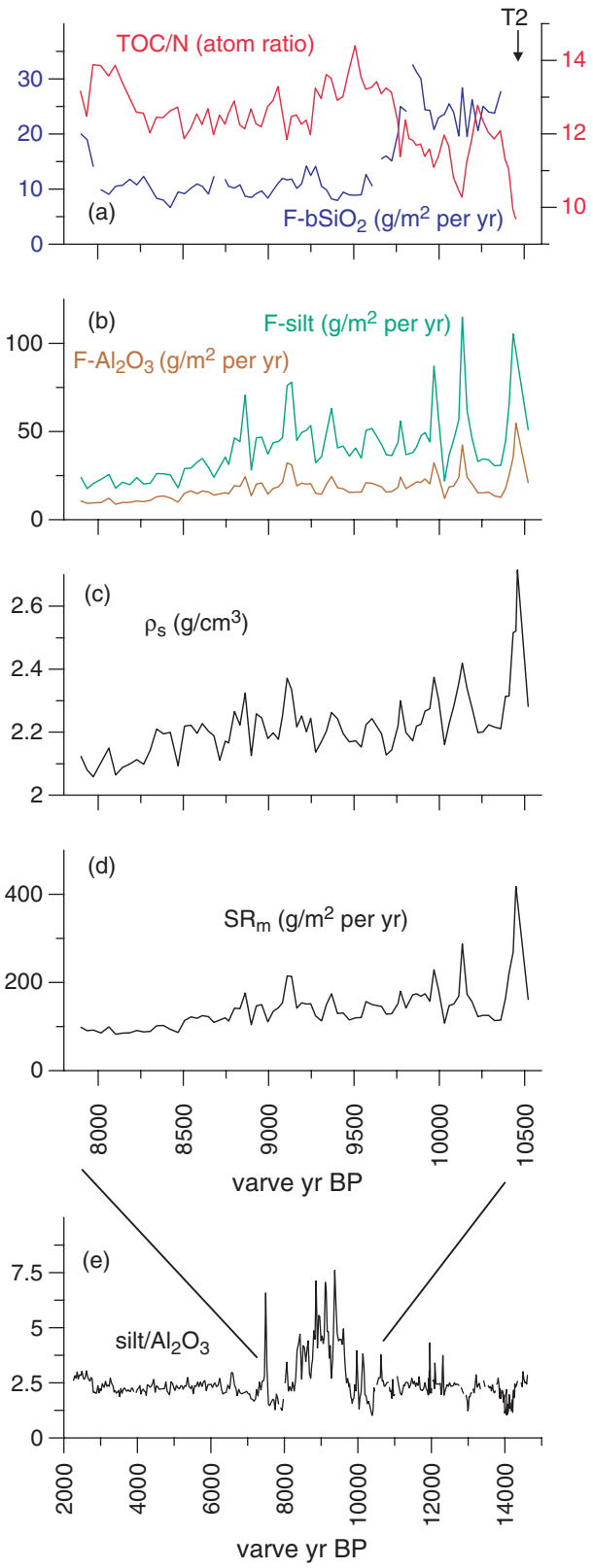

Figure 5 (a–d) Selected sedimentological and geochemical proxies that characterize Holocene sedimentation between 10 600 and 7800 varve yr BP. F-$bSiO_2$ development (a) reflects drier climatic conditions between 9500 and 8000 varve yr BP at gradually decreasing siliciclastic input (b). Dust deposition of this period is characterized by relatively higher silt contents (e). At overall substantial influx of terrestrial plant remnants, the inverse correlation between TOC/N and F-$bSiO_2$ reflects lowered proportions of terrestrial organic in the total organic sediment fraction for wetter periods with relative enhanced lake productivity

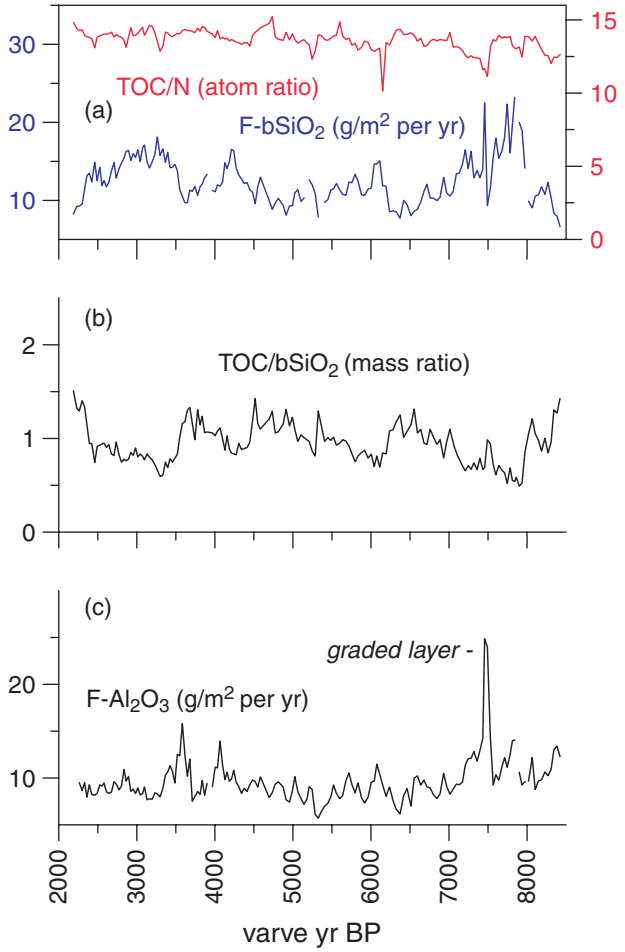

Figure 6 (a) Palaeohydrological development as implied by F-$bSiO_2$ variations for mid-Holocene sedimentation between 8000 and 2000 varve yr BP. (a,b) TOC/$bSiO_2$ and TOC/N documents relatively lowered contributions from terrestrial organic matter for wet periods with higher lake productivity. (c) Detrital influx as documented by the F-Al_2O_3 profile; siliciclastic influx shows notable peaks at the beginning and the end of a dry interval between 4000 and 3500 varve yr BP

maximum around 11 500 varve yr BP. Generally lowered TOC/N ratios of sediments deposited during this period confirm this data interpretation (Figure 2h). Flux rates of $bSiO_2$ were clearly enhanced after the fall-out of the 14-cm thick tephra layer T2 reflecting enhanced release of algae nutrients from the pumic tuff (Figure 3b). The F-$bSiO_2$ development after the tephra fall-out is therefore of minor palaeoclimatic significance without independent evidence. F-$bSiO_2$ increased again between 9900 and 9700 varve yr BP, decreased afterwards at a rather constant value of 10 g/m^2 per yr and reflects prevailing drier climatic conditions over a rather long period between 9500 and 8000 varve yr BP.

The F-Al_2O_3 profile documents declining siliciclastic influx over a period of about 75 years after the tephra fall-out (Figure 3a), F-Al_2O_3 peaks at around 10 200 and 10 000 varve yr BP are associated with enhanced atmospheric influx of silt (Figure 5b). The dry period between 9500 and 8000 varve yr BP is characterized by overall higher silt/Al_2O_3 ratios (Figure 5e). The profiles of ρ_s and SR_m reflect short-term variations in the aeolian influx of silt between 8800 and 8200 varve yr BP (compare Figure 5b,c,d). F-Al_2O_3 and F-silt gradually decrease to half of their previous background values between 9000 and 8000 varve yr BP.

8000–2000 varve yr BP

The $bSiO_2$ flux reflects increasing wetness from 8000 varve yr BP, F-$bSiO_2$ is distinctly enhanced around 7850 varve yr BP and declines afterwards to a minimum around 6500 varve yr BP (Figure 6a). Sediment sections with high F-$bSiO_2$ typically show lowered TOC/$bSiO_2$ and TOC/N values (Figure 6a,b). At overall substantial influx of terrestrial organic, as implied by the TOC/N variation range of 12 to 14, this provides independent evidence that the F-$bSiO_2$ maxima represent sedimentation intervals with enhanced deposition of planktonic matter. Sedimentation after 7500 varve yr BP is characterized by a narrower variation range of F-$bSiO_2$ (8–18 g/m^2 per yr) and an absence of graded layers, which reflects a shift to more stable hydrological conditions.

Siliciclastic input of local and remote provenance

The Ti/Al and Co/Al ratios (Figure 7a,b) reflect changes in the ratio between remote and local siliciclastic influx (Schettler *et al.*, 2006a). Enhanced influx of alkalibasaltic debris after the fallout of tephra T2 is clearly documented by distinctly enhanced Co/Al and Ti/Al values. The Ti/Al profile documents a lower proportion of local debris in the total siliciclastic influx for sedimentation before 10 000 varve yr BP when detrital influx was higher. Climate deterioration between 12 500–11 500 varve yr BP increased local soil erosion. Graded layers, deposited in this sedimentation interval, are characterized by enhanced Co/Al and Ti/Al ratios. Lateglacial sediments, deposited at high sedimentation rates after climatic amelioration between 14 300 and 13 700 varve yr BP show enhanced Co/Al only. Contributions from dissolved influx are more important for the divalent Co than for Ti. The Co/Al increase of sediments deposited around 14 000 varve yr BP may be partly associated with the leaching of Co in the catchment of the lake.

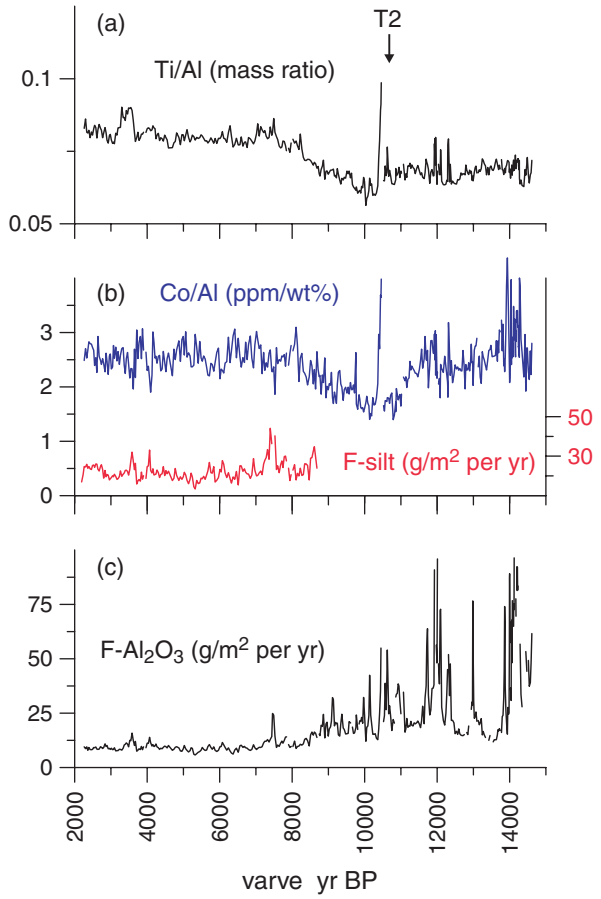

Figure 7 (a,b) Changes in the ratio between siliciclastic influx of remote and local provenance as implied by selected geochemical element ratios in the context of the total siliciclastic influx development between 15 000 and 2000 varve yr BP (c)

The profiles of Ti/Al and Co/Al furthermore imply that the proportion of local soil particles in the total allochthonous deposit declined to an absolute minimum around 10 000 varve yr BP, when F-Al_2O_3 was still more than two times higher than for sedimentation after 8000 varve yr BP (Figure 3a). Therefore, lowered influx of local debris cannot be inferred. Sediments deposited in the dry period between 9500 and 8000 varve yr BP are characterized by high silt/Al_2O_3 ratios (Figure 5a,e). In our interpretation, this reflects reduced dust influx by wet deposition together with enhanced aeolian influx of silt-sized particles by dry deposition. The proportion of the remote silicate component decreased between 10 000 and 8000 varve yr BP with a gradually decreasing siliciclastic influx after 9000 varve yr BP (Figure 7a–c). After 8000 varve yr BP the climate became wetter. The variations of Co/Al and F-$bSiO_2$ do not imply a positive correlation between summer monsoon rainfall and local soil erosion. The ratio between local and remote siliciclastics is mainly determined by variations in the atmospheric influx of silt-sized dust particles (Figure 5b–d). In the sedimentation interval 8000–2000 varve yr BP, consequently, F-silt and F-Al_2O_3 peaks coincide with Co/Al-minima (Figure 7b,c).

Relationship between summer monsoon strength and aeolian influx

Siliciclastic influx during the Lateglacial and early Holocene was generally higher than for sedimentation after 8000 varve yr BP (Figure 3a). The SHL-sediments document gradually decreasing Al_2O_3 flux from a background value of 20 g/m^2 per yr to 10 g/m^2 per yr between 9000 and 8000 varve yr BP during a period when summer monsoon rainfall in the Long Gang volcanic field, as implied by the F-$bSiO_2$ profile, was lowered (Figure 5a,b). We focus the following discussion on Holocene sedimentation between 7500 and 2000 varve yr BP without considering the event layer shortly deposited after 7500 varve yr BP. In this sedimentation interval, F-$bSiO_2$ shows relative long-term variability of the order of 100% and minor variations at century scale (Figure 8a). F-$bSiO_2$ minima do not fall below the mean F-$bSiO_2$ of the dry climate interval between 9500 and 8000 varve yr BP (Figures 5a and 8a). Individual 1-cm samples deposited between 7500 and 2000 varve yr BP represent 25 to 45 years and are characterized by $Al_2O_3/bSiO_2$ values around 0.8 and silt/Al_2O_3 ratios between 2 and 3 (Figures 2d and 5e). After *c.* 4500 varve yr BP, SR_m slightly increased on a higher background level. Enhanced SR_m is associated with an increase in autochthonous organic production and increased siliciclastic influx (Figure 3a,b).

Sediments deposited between 7500 and 4500 varve yr BP reflect significant century-scale variability of summer monsoon rainfall and document a positive correlation between F-$bSiO_2$ and siliciclastic input (F-$bSiO_2$–F-Al_2O_3, $R^2 =$ 0.473; F-$bSiO_2$–F-silt, $R^2 = 0.368$; see Figure 8f,g). The Co/Al profile does not document enhanced local soil erosion because of strengthened summer monsoon. In contrast, weak inverse correlations between F-Al_2O_3(F-$bSiO_2$) and Co/Al ($R^2 =$ 0,208(0,209)) imply a higher proportion of the remote dust component for an increase in summer rainfall (see Figure 8h for F-Al_2O_3–Co/Al). The positive correlations between F-Al_2O_3 and ρ_s ($R^2 = 0.715$, Figure 8i), and F-silt and ρ_s ($R^2 = 0.601$) document that increase of 'heavy' siliciclastic input by increase in summer monsoon rainfall exceeds the associated increase of light autochthonous biogenic deposition in this sedimentation interval.

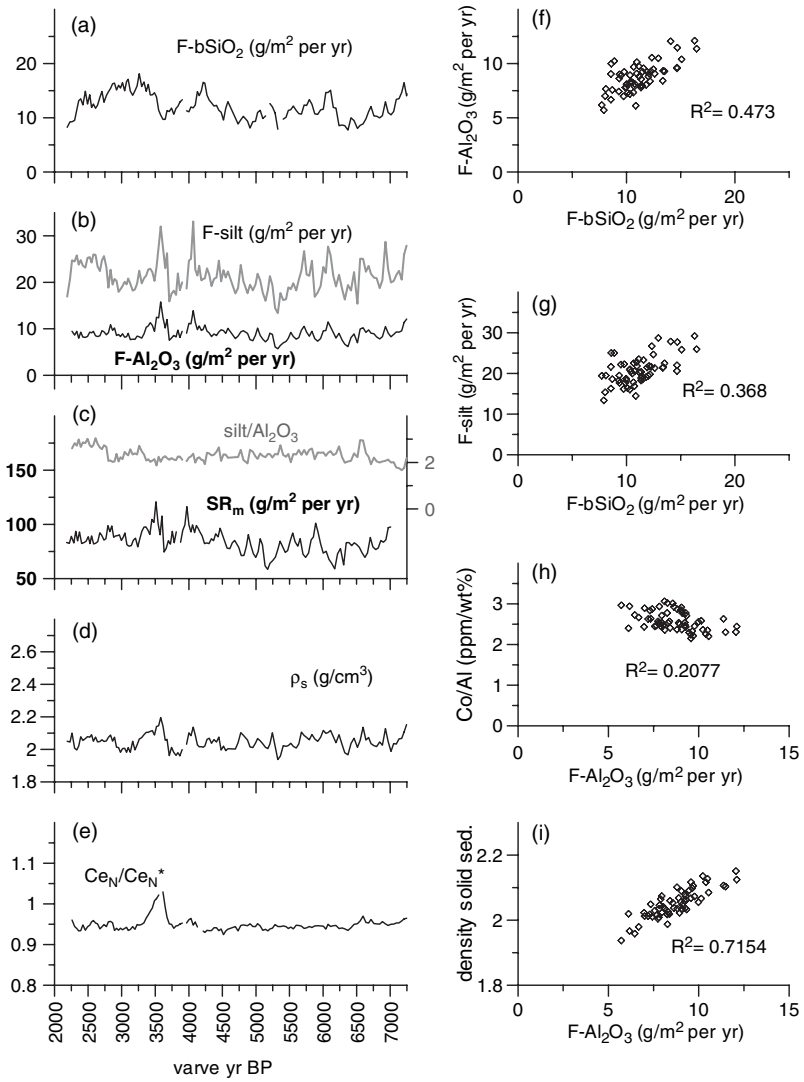

Figure 8 (a,b) Inferred East-Asian summer monsoon variability (F-$bSiO_2$) and variations in siliciclastic influx (F-Al_2O_3, F-silt). (f–i) Interval with distinct century-scale variability in summer monsoon rainfall (7300–4900 varve yr BP): Positive correlations between F-$bSiO_2$–F-Al_2O_3, and F-$bSiO_2$–F-silt of individual samples representing sedimentation between 7281 and 4874 varve yr BP reflect enhanced dust influx by wet deposition for increased summer monsoon rainfall. The proportions of local debris decrease for enhanced dust deposition (negative correlation: F-Al_2O_3–Co/Al). (d) Increase of dust influx in wet periods exceeds the increase in deposition of light biogenic matter (positive correlation: F-Al_2O_3–ρ_s). (e) Dust influx of a different provenance is detectable at the end of a dry interval around 3600 varve yr BP in the Ce_N/Ce_N* profile (ratio between normalized measured Ce_N and normalized calculated Ce_N* values ($Ce_N^* = 0.5 \cdot La_N + 0.5 \cdot Nd_N$), normalization based on mean composition of Post-Archean-Australian Shales (PAAS) for data from Taylor and McLennan, 1985).

The F-$bSiO_2$ profile reflects a strengthening of the summer monsoon after 4500 varve yr BP, temporal re-occurrence of drier conditions after *c*. 4100 varve yr BP and prevailing of wetter conditions over a rather long period between 3400 and 2350 varve yr BP. It is noteworthy that the aeolian influx shows distinct maxima at the beginning and end of the inferred dry period between 4150 and 3600 varve yr BP (Figure 8b). Enhanced seasonal aeolian input of silt over several years is documented by microscopic investigation of thin sections for the related sediment sections. Silt/Al_2O_3, however, does not show an increase in the related sediments, which implies a parallel increase in the influx of clay-sized debris. Sediments, representing sedimentation around 3600 varve yr BP, show a distinct increase of Ce_N/Ce_N* above the rather constant Ce_N/Ce_N*-background of the SHL sediments (Figure 8e). The latter implies that dust of different provenance contributed in substantial amounts to the aeolian influx. Positive Ce_N/Ce_N* values are generated in oxic top soils through percolating of rainfall and preferential retention of Ce(IV). Source regions of this dust component, therefore unlikely represent arid regions of inner Asia. They may be located west to northwest of Lake SHL close to the summer monsoon front. The distinct Ce_N/Ce_N*-peak occurs synchronously with a renewed strengthening of the summer monsoon after 3600 varve yr BP. This may reflect enhanced aeolian transport from floodplains, which may have received increased fluvial input from desertificated areas after a re-increase of the summer monsoon strength.

Comparison with modern sedimentation of Lake SHL

Table 3 compares various proxies that characterize sedimentation in Lake SHL between 8000 and 2000 varve yr BP with a historic interval (AD 1790–1953). Mean summer monsoon rainfall between AD 1790 and AD 1955, as inferred from F-$bSiO_2$, has been higher than in the mid Holocene. Subrecent sediments of Lake Sihailongwan also document distinct higher aeolian input, which exceeds the increase in

Table 3 Comparison of proxy data for modern and Holocene palaeosedimentation in Lake SHL

Parameter		1953–1790 AD	2000–8000 varve yr BP
F-bSiO$_2$ (g/m^2 per yr)	mean	22	12.8
	min	17.5	7.7
	max	27	23.2
F-Al$_2$O$_3$(g/m^2 per yr)	mean	25	9.6
	min	18.4	5.7
	max	32	24.9
SR$_m$(g/m^2 per yr)	mean	192	88
	min	146	58.5
	max	238	192
F-Al$_2$O$_3$/F-bSiO$_2$	mean	1	0.76
	min	0.9	0.46
	max	1	1.5
ρ_s(g/cm^3)	mean	2.29	2.06
	min	2.26	1.94
	max	2.34	2.39

autochthonous biogenic deposition (compare ρ_s values). In the subrecent sediments, All^{total} is adequately quantified by All^{total} = Al$_2$O$_3$ · 100/17.5 or All^{total} = 100 – bSiO$_2$ · 2.2, respectively. The higher Al$_2$O$_3$ concentration of All^{total} in the subrecent sediments reflects relatively enhanced contributions of clay-sized debris in the total dust influx. This may reflect wind erosion of fine soil particles associated with an intensification of tillage in the source regions of this dust component.

Comparison with other palaeoclimatic records

Annual rainfall in northern China shows a northwesterly declining gradient towards the modern summer monsoon limit (Figure 1). In the past, the northeasterly extension of the summer monsoon limit (SML) may have been different from the modern situation. Enhanced summer monsoon rainfall, inferred for the Long Gang volcanic field (wet periods shown in Figure 9f), must not have necessarily reached north-central China or may even have affected locations east of the modern SML. During to the prevailing of semi-arid to arid conditions in north-central China there is a general lack of highly time-resolved and continuous palaeohydrological reconstructions with reliable chronologies. In the following, however, we compare the F-bSiO$_2$ record of Lake SHL with prominent palaeoclimate records along an east–west transect from 100°E to 126°E (Figure 9a–f, see Figure 1 for sites).

Qinghai-Tibetan Plateau, Lake Qinghai, 36°32′–37°15′N, 99°36′–110°47′E, altitude 3194 m a.s.l., modern rainfall: 300 mm (Domrös and Peng, 1988); $\delta^{18}O < 9‰$ (Wei and Lin, 1998), mean $\delta^{18}O$(V-SMOW) variation range of GNIP-stations Lanzhou, Yinchuan, and Zhangye: − 6.18 to − 6.62 (Araguás-Araguás et al., 1998)

The lake receives fluvial input from *c.* 30 000 km^2 of land reaching altitudes of 4500 m a.s.l. and has no outflow. There are no signs of significant postglacial meltwater input into the lake (Figure 9a1). An ostracode oxygen isotope record (Lister *et al.*, 1991) documents the bulk effect on lake water isotope composition by changes of inflow and by variations in the evaporation/precipitation budget. The oxygen isotope profile shows a rapid negative shift after 15 000 cal. yr BP reflecting climatic amelioration and strengthening of the summer monsoon circulation. Development towards heavier isotope composition during climatic deterioration around 12 500 cal. yr BP is followed by a distinct renewed negative shift by nearly 6‰. Since *c.* 9500 cal. yr BP the oxygen isotope composition gradually changed to heavier values until *c.* 4000 cal. yr BP and remained roughly constant afterwards (Figure 9a2). In recent pollen studies (Shen *et al.*, 2005; Figure 9a2), the concentrations of total pollen, arboreal pollen, and shrub and herb vegetation is interpreted in terms of wet and dry climatic periods. The chronology of the pollen record is based on ten calibrated AMS ^{14}C datings of bulk organic matter. The Qinghai palynological record documents a humidity increase shortly before 14 000 cal. yr BP, climate deterioration around 12 000 cal. yr BP, generally wetter conditions for the first half of the Holocene and prevailing drier conditions after 4000 cal. yr BP.

Alashan Plateau, Juyan palaeolake (41°89′N, 101°85′E, 892 m a.s.l.)

The chronology of the Holocene profile is based on five calibrated AMS ^{14}C datings of bulk organic material. Herzschuh *et al.* (2004) infer variations in precipitation applying quantitative and semi-quantitative approaches, best modern analogue approach (BMA), the numerical biome scores and the ratios of *Artemisia*/Chenopodiaceae and *Ephedra distachya*-type/*Ephedra fragilis*-type pollen. In particular, inferred change between wet and dry conditions for the period between 5000 and 2000 cal. yr BP shows similarity with the F-bSiO$_2$ profile development of Lake SHL.

Ordos Plateau (Inner Mongolia), Lake Yanhaizi (40°06′–40°10′N, 108°25′E–108°29′E, 1180 m a.s.l.)

Lake Yanhaizi is a hyper-saline shallow lake with a catchment area of 2000 km^2. Mean annual evaporation of 2604 mm distinctly exceeds modern annual rainfall of 227 mm. Chronostratigraphy of the sedimentation record is based on a total of ten calibrated AMS ^{14}C dates of TOC, humin and pollen. Chen-Tung *et al.* (2003) reconstruct wet and dry periods based on TOC and changes in grain size composition. The authors interpret sediment sections where coarse particle sizes dominate as arid phases, sections with enhanced TOC as wet periods. The TOC profile implies a 1500 yr dry interval between 9000 and 7500 cal yr BP, which seems to be slightly out of phase with the dry period inferred from the SHL sediments (9500–*c.* 8000 varve yr BP). According to the authors' data interpretation of grain size composition, however, a shift to wet conditions could already have occurred around 8000 cal. yr BP. Development towards wetter conditions and precipitation decline to a minimum around 5000 cal. yr BP, as well as wetness increase around 4200 cal. yr BP show some similarity with the palaeohydrological reconstruction of Lake SHL. Grain size composition in the sedimentation interval 3500–2500 cal. yr BP indicates overall wet conditions that might be camouflaged in the TOC concentration profile by increased detrital influx (human impact).

Lake Daihai, (Inner Mongolia), 40°29′–40°37′N, 112°33′–112°46′E, 1221 m a.s.l.

The lake receives inflow from five major rivers and has no outflow. Holocene chronostratigraphy is based on seven calibrated AMS ^{14}C dates of TOC. (Figure 9d1) The palynological record of the lake (Xiao *et al.*, 2004) documents increased wetness after *c.* 8000 cal. yr BP and drier conditions around 2000 cal. yr BP. Similar to the palaeohydrological reconstruction of Lake SHL, pollen data of Lake Daihai sediments reflect humidity variations between 8000 and 3000 cal. yr BP at millennial scale (Figure 9d2). Peng *et al.* (2005)

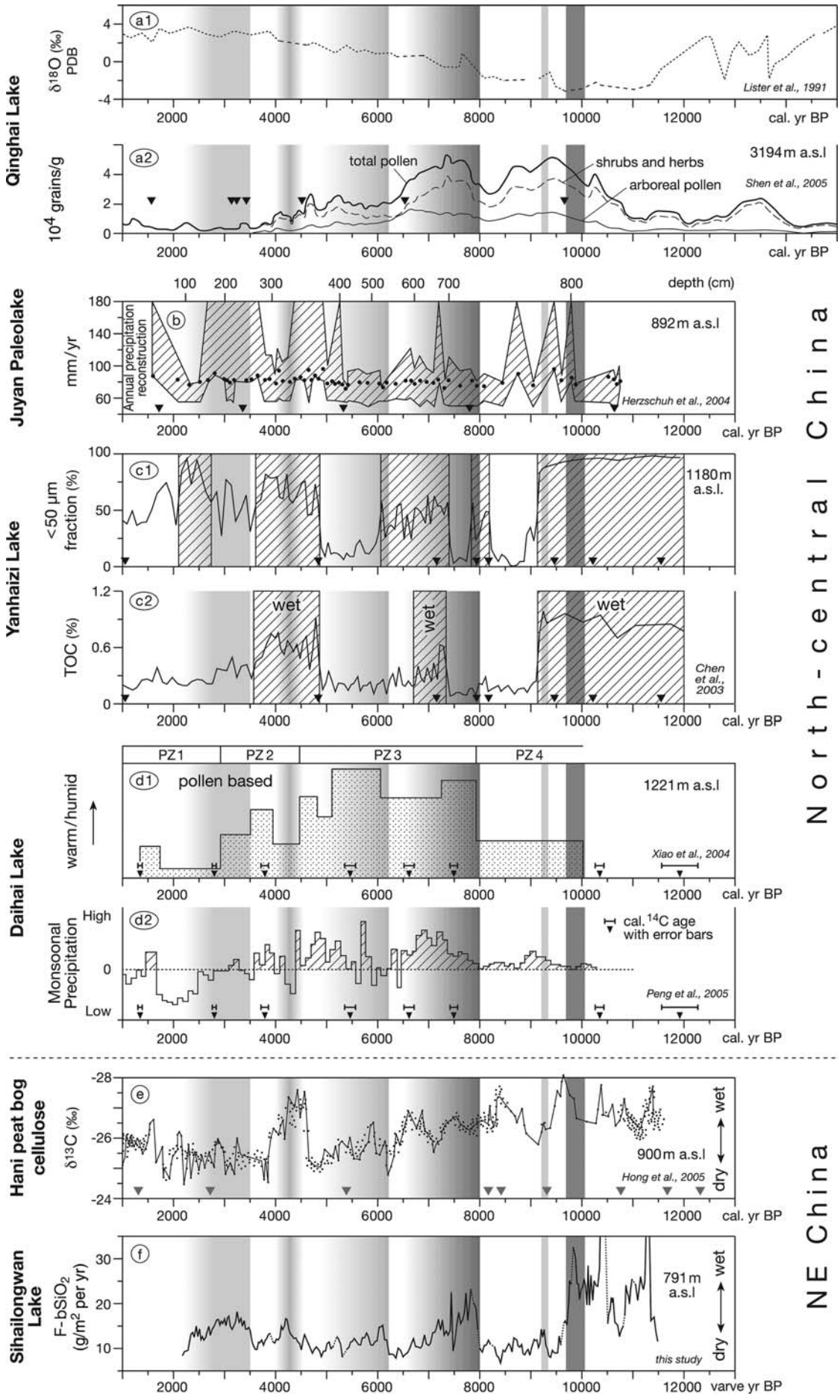

Figure 9

interpret an increase in mean grain size as an indication for enhanced fluvial influx and increased precipitation in the region, respectively. In particular, prevailing relatively dry conditions until *c.* 8000 cal. yr BP and distinctly reduced wetness around 2000 cal. yr BP are indicated by this proxy.

Hani peat profile (Jilin province), 42°13′N, 126°13′E, 900 m a.s.l., close to Lake SHL

The chronology of the 8-m peat profile is based on calibrated AMS-^{14}C dates of a total of ten specimens of peat cellulose and an assumed constant rate of peat growth. The δ^{13}C value of peat cellulose, which originates exclusively from C3-plants, is interpreted by Hong *et al.* (2001) as a proxy for local climatic wetness, with negative shifts of δ^{13}C implying higher soil moisture or precipitation (see White *et al.*, 1994, for the theoretical background of the relationship). The carbon isotope data from the peat profile imply a relatively short duration of the dry periods around 9000 and 2000 cal. yr BP. This may be related to decreased peat accumulation for drier climatic conditions.

Comparison of the palaeohydrological reconstruction of Lake SHL (Figure 9f) with the mid-latitudinal proxy records from north-central China between 37° and 42° N reviewed above, documents that climate change to warmer and moister conditions in northeast China around 14 300 cal. yr BP occurred nearly synchronously with climatic amelioration in arid areas close to the modern summer monsoon front (Figures 3b,d and 9a2). A Younger Dryas-like climatic deterioration documented in the SHL sediments by pollen and geochemical proxy data (Figures 3c, 4a), is also documented in palaeoclimatic records from southern China and Japan (Dykoski *et al.*, 2005; Mingram *et al.*, 2004a; Wang *et al.*, 2001; Nakagawa *et al.*, 2002, 2003). An inferred early Holocene maximum in summer monsoon circulation shortly after 10 000 cal. yr BP, which is supported by independent proxy data from the nearby Hani peat profile (Figure 9e,f), probably also affected north-central China (Figure 9a1,e,f). There are indications for a weakening of the East-Asian summer monsoon strength in a sedimentation interval between 9500 and 8000 cal. yr BP (see Figure 9f for Lake SHL), particularly, in the proxy records from Lake Yanhaizi, Lake Daihai, Lake Qinghai and the Hani peat profile. The synchrony regarding the onset and duration of the dry period has to be seen in the light of the chronologies of these records, which are based on linear depth–age interpolations between very few radiometric ^{14}C-datings (mainly of bulk organic material). There is high correspondence in most of the referred records regarding the abrupt shift to a wetter climate around 8000 cal. yr BP and a gradual weakening of the East-Asian summer monsoon until 6200 cal. yr BP. The inferred rapid strengthening of the summer monsoon at 6000 cal. yr BP with gradually declining precipitation afterwards, as documented in the SHL, Hani and Dahai records, seems not to have affected north-central China west of 110°E (Figure 9a,b,c). Re-strengthening of the East-Asian summer monsoon around 4200 cal. yr BP (Figure 9f), which finds strong response in the proxy data from the Hani peat, is also indicated in the proxy records from Palaeolake Juyan and Lake Yanhaizi. The inferred distinct dry interval shortly after 4000 cal. yr BP is indicated in all records. Huang *et al.* (2004), An *et al.* (2005) and references therein, give archaeological evidence for a collapse of rain-fed agriculture cultures on the western Loess Plateau shortly after 4000 cal. yr BP and discuss this as result of climatic deterioration. The F-bSiO_2 profile development of Lake SHL for this period reflects a distinct weakening of the East-Asian summer monsoon and sustains such an interpretation. Vegetation development in the Qinghai Lake area shows only weak reflection on the distinct summer monsoon strengthening around 4200 cal. yr BP and no response for the inferred wet interval between 3500 and 2200 cal. yr BP. The inferred shift to drier conditions (Figure 9f) around 2000 cal. yr BP is particularly well recorded in the proxy data from Palaeolake Juyan, Lake Dahai and the Hani peat profile (Figure 9b,d1,d2,e).

Summary

Reconstructed Holocene net accumulation rates of biogenic silica imply that summer monsoon rainfall reached maxima in the early Holocene around 9800 and 7800 cal. yr BP. Groundwater inflow during these periods, however, probably did not reach the level of the subsurface drainage from the catchment during the Lateglacial warm period (*c.* 14 300–12 500 varve yr BP) and after the end of a Younger Dryas-like climatic deterioration when the evapotranspiration in the lake catchment was relatively lower because of less dense woody vegetation cover. Summer monsoon rainfall was reduced between 9500 and 8000 cal. yr BP and reached minima around 6400, 4900, 3700 and around 2200 varve yr BP. Derived flux rates for the dissolved Mo input (F-Mo^{exc}) give independent evidence for a distinct increase of groundwater inflow after 14 300 varve yr BP, lowered groundwater inflow between 12 500 and 11 500 varve yr BP, high groundwater inflow around 10 300 varve yr BP and gradually decreasing subsurface inflow afterwards. F-bSiO_2 development between 8000 and 2000 varve yr reflects minor short-term variability at century-scale and major millennial-scale variations in the amount of summer monsoon rainfall.

Aeolian siliciclastic influx has been generally higher before 8000 varve yr BP than for the period afterwards. In a mid-Holocene sedimentation interval with distinct century-scale F-bSiO_2 variability (7300–4300 varve yr BP), F-bSiO_2 and F-Al_2O_3 are positively correlated, which reflects enhanced dust influx resulting from increase of summer monsoon rainfall at an overall high dust load over the Asian continent. Remarkably, aeolian influx peaked at the onset and at the end of a

Figure 9 (a–f) Compilation of palaeoclimatic records from north-central and northeast China along a *c.* 2000 km east–west transect that document changes in the East-Asian summer monsoon strength (see Figure 1 for locations, explanations are given in Section 'Comparison with other palaeoclimate records'. Depth positions of calibrated AMS ^{14}C-datings are marked by triangles inside the diagrams, inferred wet intervals of referred records marked by diagonal hatching, wet periods inferred in this study are marked by shaded columns across all diagrams. (a) Ostracode oxygen isotope record, initial data of Lister *et al.* (1991), redrawn at calibrated age scale by Wei and Gasse (1999). (b) Annual precipitation reconstruction from pollen data using BMA approach: most probable values (circles) are based on the weighted average of the selected analogues and confidence intervals (lines) taken from the climatic distribution of the selected analogues. (c1) Sedimentation intervals with dominance of coarse particles are interpreted as dry periods by the authors. (d1) PZ4: mild and dry climate implied by dominance of arid herbs and shrubs with patches of pine and broadleaved forests, PZ3: large-scale covers of mixed coniferous and broadleaved forests, PZ2 decline of arboreal pollen implies development towards cooler and drier conditions, PZ1 disappearance of forests reflects drier conditions. (d2) Inferred from surface inflow reconstructions based on grain size data

dry interval between 4100 and 3600 cal. yr BP. Sediments deposited around 3600 cal. yr. BP document dust influx of different geochemical provenance. Mean annual mass accumulation between 7000 and 2000 varve yr BP accounts for only 46% of the inferred mean SR_m value of a 163-yr subrecent sedimentation period between AD 1790 and AD 1953. Increased sediment accumulation in the last two centuries reflects higher autochthonous production, in together with higher aeolian influx (F-$bSiO_2$ increase: 1.7 times, F-Al_2O_3 increase: 2.6 times). The siliciclastic sediment constituent of modern SHL sediments is about 17.5 wt%, reflecting higher contributions from clay-sized dust particles. Dust influx from other source regions may have become important by human impact at remote areas in the historic period.

Acknowledgements

We acknowledge support by technicians of the GFZ-Potsdam, Section 'Climate Dynamics and Sediments': Andreas Hendrich (drawing of figures), Ursula Kegel and Stefan Adler (analytical assistance), Dieter Berger and Michael Köhler (drilling and thin section preparation). Drilling and extensive laboratory work was financed by the GFZ-Potsdam in the framework of the German-Chinese Science co-operation. Qiang Liu thanks for the support from the National Basic Research Program of China (No. 2004CB720207) and the National Natural Science Foundation of China (Grant No. 40302023). Dr Chu Guoqing and Ni Yunyan are thanked for their help in organizing the field work. We thank Professor J.F.W. Negendank and Professor Liu Jiaqi who initiated the lake studies in the Long Gang volcanic field, Dr O. Bothe (University of Hamburg) for guidance on the field of meteorology, and Dr D. Harlov for checking the English. We thank Dr Yiyin Li (Long-term Ecology Laboratory, University of Oxford) and an anonymous reviewer for helpful comments to improve the manuscript.

References

An, C.-B., Tang, L., Barton, L. and **Chen, F.H.** 2005: Climate change and cultural response around 4000 cal yr. BP in the western part of Chinese Loess Plateau. *Quaternary Research* 63, 347–52.

An, Z., Porter, S.C., Kutzbach, J.K., Xihao, W., Suming, W., Xiadong, L., Xiaoqiang, L. and **Weijian, Z.** 2000: Asynchronous Holocene optimum of the East Asian monsoon. *Quaternary Science Reviews* 19, 743–62.

Araguás-Araguás, L., Froehlich, K. and **Rozanski, K.** 1998: Stable isotope composition of precipitation over southeast Asia. *Journal Geophysical Research* 103, D22, 28 721–42.

Barry, R.G. and **Chorley, R.J.** 1998: *Atmosphere, weather and climate*. 7th edition. Routledge.

Bruno, J., De Pablo, J., Duro, L. and **Figuerola, E.** 1995: Experimental study and modelling of the U(VI)-Fe$(OH)_3$ surface precipitation/co-precipitation equilibria. *Geochimica Cosmochimica Acta* 59, 4113–23.

Bush, A.B.G. 2001: Pacific sea surface temperatures forcing dominates orbital forcing of the early Holocene Monsoon. *Quaternary Research* 55, 25–32.

—— 2005: CO_2/H_2O and orbitally driven climate variability over central Asia through the Holocene. *Quaternary International* 136, 15–23.

Chen-Tung, A.Ch., Lan, H.-Ch., Lou, J.-Y. and **Chen, Y.Ch.** 2003: The dry Holocene megathermal in Inner Mongolia. *Palaeogeography Palaeoclimatoloy Palaeoecology* 193, 181–200.

Chu, G., Liu, J., Schettler, G., Li, J., Sun, Q., Gu, Z., Lu, H., Liu, Q. and **Liu, T.** 2005: Sediment fluxes and varve formation in Sihailongwan, a maar lake from northeastern China. *Journal of Paleolimnology* 34, 311–24.

Davis, J.A., Meece, D.E., Kohler, M. and **Curtis, G.P.** 2004: Approaches to surface complexation modeling of Uranium(VI) adsorption on aquifer sediments. *Geochimca Cosmochimica Acta* 68, 3621–41.

Domrös, M. and **Peng, G.** 1988: *The climate of China*. Springer, 360 pp.

Dykoski, C.A., Edwards, R.L., Cheng, H., Yuan, D., Cai, Y., Zhang, M., Lin, Y., Qing, J., An, Z. and **Revenaugh, J.** 2005: A high-resolution, absolute-dated Holocene and deglacial Asian monsoon record from Dongge Cave, China. *Earth Planetary Science Letters* 233, 71–86.

Gao, Y.X., Xu, S.Y., Guo, Q.Y. and **Zhang, M.L.** 1962: Monsoon regions in China and regional climates. In Gao, Y.X., editor, *Some problems on East-Asia monsoon.* Science Press, 49–63 (in Chinese).

He, Y., Theakstone, W.H., Zhonglin, Z., Dian, Z., Tandong, Y., Tuo, Ch., Shen, Y. and **Hongxi, P.** 2004: Asynchronous Holocene climate change across China. *Quaternary Research* 61, 52–63.

Herzschuh, U., Tarasov, P., Wünnemann, B. and **Hartmann, K.** 2004: Holocene vegetation and climate of the Alashan Plateau, NW China, reconstructed from pollen data. *Palaeogeography Palaeoclimatology Palaeoecology* 211, 1–17.

Hong, Y.T., Wang, Z.G., Jiang, H.B., Lin, Q.H., Hong, B., Zhu, Y.X., Wang, Y., Xu, L.S., Leng, X.T. and **Li, H.D.** 2001: A 6000-year record of changes in drought and precipitation in northeastern China based on $\delta^{13}C$ time series from peat cellulose. *Earth Planetary Science Letters* 185, 11–119.

Hong, Y.T., Hong, B., Lin, Q.H., Shibata, Y., Hirota, M., Zhu, Y.X., Leng, X.T., Wang, Y., Wang, H. and **Yi, L.** 2005: Inverse phase oscillations between the East Asian and Indian Ocean summer monsoons during the last 12 000 years and paleo-El Niño. *Earth Planetary Science Letters* 231, 337–46.

Hu, Z.-Z. 1997: Interdecadal variability of summer climate over East Asia and its association with 500hPa height and global sea surface temperature. *Journal Geophysical Research* 102, D16, 19 403–12.

Huang, C.C., Pang, J., Zhou, Q. and **Chen, S.** 2004: Holocene pedogenic change and the emergence and decline of rain-fed cereal agriculture on the Chinese Loess Plateau. *Quaternary Science Reviews* 23, 2525–35.

Kudrass, H.R., Erlenkeuser, H., Vollbrecht, R. and **Weiss, W.** 1991: Global nature of the Younger Dryas cooling event inferred from oxygen isotope data from the Sulu Sea cores. *Nature* 349, 406–409.

Kumar, K.K., Rajagopalan, B. and **Cane, M.A.** 1999: On the weakening relationship between the Indian Monsoon and ENSO. *Science* 284, 2156–59.

Kutzbach, J.E. 1981: Monsoon climate of the early Holocene: climate experiment with the Earth's orbital parameters for 9000 years ago. *Science* 214, 59–61.

Lister, G.S., Kelts, K., Chen, K., Yu, J. and **Niessen, F.** 1991: Lake Qinghai, China: closed-basin lake levels and the oxygen isotope record of ostracoda since the latest Pleistocene. *Palaeogeography Palaeoclimatology Palaeoecology* 84, 141–62.

Merkt, J. 1971: Zuverlässige Auszählungen von Jahresschichten in Seesedimenten mit Hilfe von Großdünnschliffen. *Archiv für Hydrobiologie* 69, 145–54.

Mingram, J., Schettler, G., Nowaczyk, N., Luo, X., Lu, H., Liu, J. and **Negendank, J.F.W.** 2004a: The Huguang maar lake – a high-resolution record of palaeoenvironmental and palaeoclimatic changes over the last 78,000 years from South China. *Quaternary International* 122, 85–107.

Mingram, J., Allen, J.R.M., Brüchmann, C., Liu, J., Luo, J., Negendank, J.F.W., Nowaczyk, N. and **Schettler, G.** 2004b: Maar- and crater lakes of the Long Gang Volcanic FIeld (N.E. China) – overview, laminated sediments, and vegetation history of the last 900 years. *Quaternary International* 123–125, 123–47.

Morrill, C., Overpeck, J.T. and **Cole, J.E.** 2003: A synthesis of abrupt changes in the Asian summer monsoon since the last deglaciation. *The Holocene* 13, 465–76.

Nakagawa, T., Tarasov, P.E., Nishida, K., Gotanda, K. and **Yasuda, Y.** 2002: Quantitative pollen-based climate reconstruction in

central Japan: application to surface and Late Quaternary spectra. *Quaternary Science Reviews* 21, 2099–113.

Nakagawa, T., Kitagawa, H., Yasuda, Y., Tarasov, P.E., Nishida, K., Gotanda, K., Sawai, Y. and **Yangtze River Civilization Program Members** 2003: Asynchronous Climate Changes in the North Atlantic and Japan During the Last Termination. *Nature* 299, 688–91.

Peng, Y., Xiao, J., Nakamura, T., Liu, B. and **Inouchi, Y.** 2005: Holocene East Asian monsoonal precipitation pattern revealed by grain-size distribution of core sediments of Daihai Lake in Inner Mongolia of north-central China. *Earth Planetary Science Letters* 233, 467–79.

Reimer, P.J., Baillie, M.G.L., Bard, E., Bayliss, A., Beck, J.W., Bertrand, Ch.J.H., Blackwell, P.G., Buck, C.E., Burr, G.S., Cutler, K.B., Damon, P.E., Edwards, R.L., Fairbanks, R.G., Friedrich, M., Guilderson, Th.P., Hogg, A.G., Hughen, K.A., Kromer, B., McCormac, G., Manning, St., Ramsey, Chr.B., Reimer, R.W., Remmele, S., Southon, J.R., Stuiver, M., Talamo, S., Taylor, F.W., van der Plicht, J. and **Weyhenmeyer, C.E.** 2004: IntCal04 terrestrial radiocarbon age calibration, 0–26 cal kyr BP. *Radiocarbon* 46, 1029–58.

Schettler, G., Liu, Q., Mingram, J. and **Negendank, J.F.W.** 2006a: Paleovariations in the East-Asian Monsoon regime geochemically recorded in varved sediments of Lake Sihailongwan (Northeast China). Part 1: hydrological conditions and dust flux. *Journal Paleolimnology* 35, 239–70.

Schettler, G., Mingram, J., Negendank, J.F.W. and **Jiaqi, L.** 2006b: Palaeovariations in the East-Asian Monsoon regime geochemically recorded in varved sediments of Lake Sihailongwan (Northeast China, Jilin province). Part 2: a 200 year record of atmospheric lead-210 flux variations and its palaeoclimatic implications. *Journal Paleolimnology* 35, 271–88.

Shen, J., Liu X., Wang, S.W. and **Matsumoto, R.** 2005: Palaeoclimatic changes in the Qinhai Lake area during the last 18,000 years. *Quaternary International* 136, 131–40.

Stebich, M., Arlt, J. and **Mingram, J.** 2007: Late Quaternary vegetation history of N.E.-China–recent progress in the investigation of Sihailongwang maar lake. In Kahlke, R.-D., Maul, L.C. and Mazza, P., editors, Late Neogene and Quaternary biodiversity and evolution: regional developments and interregional correlations. *Proceedings of the 18th International Senckenberg Conference (VI International Palaeontological Colloquium in Weimar), Courier Forschungsinstitut Senckenberg*. Nägele und Obermiller, in press.

Taylor, S.R. and **McLennan, S.M.** 1985: *The continental crust: its composition and evolution*. Blackwell, 312 pp.

Tribovillard, N., Riboulleau, A., Lyons, T. and **Baudin, F.** 2004: Enhanced trapping of molybdenum by sulfurized marine organic matter of marine origin in Mesozoic limestones and shales. *Chemical Geology* 213, 385–401.

Vorlicek, P.T., Kahn, M.D., Kasuya, Y. and **Helz, G.R.** 2004: Capture of molybdenum in pyrite-forming sediments: role of ligand-induced reduction by polysulfides. *Geochimica Cosmochimica Acta* 68, 547–56.

Wang, P., Clemens, S., Beaufort, L., Braconnot, P., Ganssen, G., Jian Z., Kershaw, P. and **Sarntheim, M.** 2005: Evolution and variability of the Asian monsoon system: state of the art and outstanding issues. *Quaternary Science Reviews* 24, 595–629.

Wang, Y.J., Cheng, H., Edwards, R.L., An, Z.S., Wu, J.Y., Shen, C.-C. and **Dorale, J.A.** 2001: A high-resolution absolute-dated Late Pleistocene monsoon record from Hulu Cave, China. *Science* 294, 2345–48.

Wei, K. and **Gasse, F.** 1999: Oxygen isotopes in lacustrine carbonates of West China revisited: implications for post glacial changes in summer monsoon circulation. *Quaternary Science Reviews* 18, 1315–34.

Wei, K. and **Lin, R.** 1998: Isotope geochemistry of meteoric waters, In Tu, G.Z., Chou, T.Z., Yu, J.S., Chen, Y.W. and Li, Y.S., editors, *Isotope geochemistry research in China*. Section VI, Chapter 25. Science Press, 443–64.

White, J.W.C., Ciais, P., Figge, R.A., Kenny, R. and **Markgraf, V.** 1994: A high-resolution record of atmospheric CO_2 content from carbon isotopes in peat. *Nature* 367, 153–56.

Xiao, J., Xu, Q., Nakamura, T., Yang, X., Liang, W. and **Inouchi, Y.** 2004: Holocene vegetation variation in the Daihai Lake region of north-central China: a direct indication of the Asian monsoon climatic history. *Quaternary Science Reviews* 23, 1669–79.